Influence of Excess Fuel from Timber Lined Compartments

Influence of Excess Fuel from Timber Lined Compartments

Nomenclature

A_B	Burning area (m^2)
A_V	Ventilation area (m^2)
C	Oxygen flow constant ($kg/s.m^{5/2}$)
C_d	Discharge coefficient (-)
f	Excess fuel factor (-)
g	Gravitational constant (m/s^2)
h_0	Neutral plane height (m)
H_V	Ventilation height (m)
$\dot{m}$	Mass loss rate (kg/s)
$\dot{Q}$	Heat release rate (kW)
r	Stoichiometric air:fuel ratio (-)
W_V	Ventilation width (m)
ΔH_c	Heat of combustion (kJ/g)
κ	Fuel-specific constant ($kg/s.m^{5/2}$)
ρ	Density (kg/m^3)
χ	Combustion efficiency (-)
ϕ	Global Equivalence Ratio (-)

Subscripts

a	Air
b,e	Burning, external
b,i	Burning, internal
g	Gases
p	Pyrolysis

Abstract

External fire spread is a key risk faced by engineers in the design of buildings. This can be quantified by heat flux to an exposed surface, which is dependent on the conditions in the external fire plume. Introducing additional fuel in the form of exposed timber surfaces is shown to increase the energy released by external flaming, as defined by an excess fuel factor or Global Equivalence Ratio (GER). This paper presents a review of three recent experimental series exploring the effects of exposed timber on compartment fire dynamics, and uses experimental data to calculate the GER for each experiment. When combustion efficiency was assumed equal to one, Global Equivalence Ratios were found to range from 0.58 to 3.00; these corresponded to a compartment with a single exposed timber surface and a compartment with three exposed timber surfaces. A “burning factor” has been introduced to as a possible method to relate GER to the properties of the compartment. It is found that a relatively good correlation (R^2>0.9) is achieved between burning factor and GER when only the compartment surfaces are burning, but that the correlation does not hold when other fuel load is also burning within the compartment.

1. Introduction

External fire spread is one of the key risks that engineers and authorities attempt to address during the design of buildings. There are typically two objectives with respect to external fire spread: 1) limit the vertical spread on the surface external envelope of a building or between compartmentalised floors; 2) limit the fire spread to or from adjacent buildings. To address these objectives, there are a variety of engineering tools. Each of these are based on the fundamental idea that the heat flux to the exposed surface (i.e. adjacent building, or upper storey) should be limited. Spandrel panels, protruding balconies, and space separation are all techniques that are used to limit external fire spread. Spandrel panels introduce a vertical gap between combustible materials on different floors (thereby reducing the heat flux to new sources of fuel); protruding balconies introduce a horizontal gap between the fire plume and the vertically adjacent compartment (thereby reducing the heat flux to new sources of fuel); and space separation to adjacent building reduces the view factor (and therefore the incident heat flux on nearby buildings).

Inherent within each of these engineering techniques are assumptions about the compartment fire behaviour. Most engineering methods are based on quantification of the heat flux from a fully developed compartment fire (as opposed to a fire with an external source). In the case of vertical fire spread from a compartment fire, it is the heat flux from the external plume to upper floors that must be addressed. In the case of lateral fire spread (to adjacent buildings), the combination of heat flux from within the compartment (i.e. from the openings) and from the fire plume must be addressed. There are therefore two primary considerations for addressing this risk: the heat flux from the plume (through radiation and convection), and the heat flux from the compartment opening (dominated by radiation).

The heat flux resulting from the external plume is closely linked to the fire dynamics within a fully developed fire – the plume behaviour is a function of the opening geometry (width, height, ventilation factor), the heat release rate of the fire, and the fuel properties [1]. Of particular importance for the external plume is the amount of fuel that is available to combust in the plume. In a ventilation controlled fire, there is insufficient oxygen within the compartment to burn all of the fuel. Consequently, some of the fuel is burned outside the compartment – resulting in external flaming. The quantity of fuel burned outside the compartment (and therefore the heat flux due to the external fuel) can be quantified by the excess fuel factor. The excess fuel factor and its application to external flaming was first established by Bullen and Thomas [2].

Timber lined compartments associated with the use of exposed Cross-Laminated Timber (CLT) introduce additional fuel area into a compartment. Consequently, the area over which

pyrolysis occurs will be greater, thus allowing for an increased pyrolysis rate (note the internal burning rate will still be limited by the availability of oxygen). This has the potential to significantly increase the unburnt fuel exiting the compartment – and hence the excess fuel factor. The impact of this increased fuel area on the potential for external fire spread (both vertical and horizontal) has, to date, received relatively little attention in the literature.

This paper presents a review of recent large-scale experimental work on compartments with exposed timber surfaces. The intent is to identify the characteristic range of excess fuel factor that may result from a timber-lined compartment – thereby informing future research in this area.

2. Background

2.1. The Excess Fuel Factor/Global Equivalence Ratio

Research into compartment fire behaviour has consistently shown that the rate of burning inside a fire compartment is controlled by the available oxygen, and hence the ventilation conditions. The mass of available oxygen can be calculated as a function of the opening geometry for ventilation-controlled fires [1, 3]:

$$\dot{m}_a = 0.5 A_v \sqrt{H_v} \tag{1}$$

where $\dot{m}_a$ is the mass of air entering the compartment, A_v is the opening area, and H_v is the opening height. Equation 1 has no dependence on the fuel load or configuration, and thus the mass of oxygen entering the compartment is limited purely by the opening geometry. This limits the amount of burning which can take place inside the compartment, $\dot{m}_{b,i}$. This can be expressed as a function of the airflow in and the stoichiometric air to fuel ratio, r:

$$\dot{m}_{b,i} = \frac{\dot{m}_a}{r} = \frac{0.5 A_v \sqrt{H_v}}{r} \tag{2}$$

This can then be expressed as (e.g [3]).:

$$\dot{m}_{b,i} = \kappa A_v \sqrt{H_v} \tag{3}$$

where κ is a fuel-specific constant – for example, 0.09 for wood [3].

This should not be conflated with the rate at which the fuel pyrolyses, $\dot{m}_p$ which has been shown to be dependent on the heat provided to the fuel surface from the hot gases and flames [4]. This can result in a pyrolysis rate that is greater than the burning rate inside the compartment. In the case of exposed CLT surfaces, the pyrolysis rate will increase due to the increased fuel surface area – however the burning rate inside the compartment will still be limited by available oxygen.

Excess fuel which is unable to burn inside the compartment will leave the compartment with the exhaust gases from the fuel burning inside the compartment. Much of this excess fuel will burn in the external plume (where there is available oxygen). The mass of fuel available to burn in this external plume can thus be calculated as:

$$\dot{m}_{b,e} = \dot{m}_p - \dot{m}_{b,i} \tag{4}$$

The excess fuel can be expressed as a ratio of the total pyrolysis rate to the maximum burning rate inside the compartment. This is defined as a "Global Equivalence Ratio" (GER) [5], and is defined for a compartment as:

$$\phi = \frac{\dot{m}_p r}{\dot{m}_a} \tag{5}$$

where the stoichiometric ratio of air to fuel for wood is 5.7 [1]. A key underlying assumption of this value is that complete combustion occurs – this will not be the case in a real fire. Even in cases where there is sufficient oxygen entering the compartment to burn all the fuel (thus a GER equal to or less than one), some unburned gases (and some oxygen) may still leave through the compartment opening due to inadequate mixing. These gases will then burn outside the compartment. The inadequate mixing will also result in reduced combustion efficiencies within the compartment [6].

The excess burning can also be characterised by using the index of an "excess fuel factor" [2], which is the fraction of fuel burned outside the compartment:

$$f = \frac{\dot{m}_{b,e}}{\dot{m}_p} = 1 - \frac{\dot{m}_{b,i}}{\dot{m}_p} \tag{6}$$

which can be expanded into:

$$f = 1 - \frac{\dot{m}_a}{r\dot{m}_p} \tag{7}$$

This can be related to the GER as:

$$\phi = \frac{1}{1-f} \tag{8}$$

The GER is therefore an indication of the amount of unburnt fuel exiting the compartment. A GER of zero implies that there is no burning, whereas a GER of unity implies perfect stoichiometry and thus no unburnt fuel exiting the compartment. A GER >1 will result in more fuel exiting the compartment. It follows from this that an increased GER represents a greater hazard in terms of external flaming and resulting heat flux to upper storeys and to adjacent buildings. The excess fuel factor expresses the same phenomena: zero implies stoichiometry; a negative value indicates that all fuel is burned inside the compartment; and a positive value implies unburnt fuel leaving the compartment.

From these equations it can be concluded that if the rate of pyrolysis increases, then the GER (and resulting external heat fluxes from external burning) will also increase. This was a key finding of Bullen [2]. However, at the time when Bullen was working it was assumed that most fuel would be located on the compartment floor. Relatively little attention was therefore given to the effect of the presence of combustible linings on the walls or ceiling. The use of exposed CLT introduces fuel onto the walls and/or ceiling of the compartment. It follows from this that increases will occur in the overall pyrolysis rate in the compartment, the GER, and the resulting heat fluxes from the plume [7].

2.2. Calculation of Global Equivalence Ratio

To estimate the Global Equivalence Ratio (GER) for a compartment, it is necessary to know the mass of air entering the compartment. The literature demonstrates that mass flow into the compartment can be estimated by Equation 1 [1, 3], reformulated below:

$$\dot{m}_a = CA_v\sqrt{H_v} \tag{9}$$

This is a simplified expression based on the following assumptions:

1) Ambient density is 1.2 kg/m^3;
2) The ratio of ρ_a/ρ_g lies between 1.8 and 5 (i.e. outflow temperature is between ~250°C and ~1200°C);
3) The discharge coefficient, C_d, is 0.7;
4) Mass flow in and mass flow out are equal – which implies a burning rate of zero (this results in the assumption that the ratio ϕ/r_a is equal to zero).

Each of these assumptions has varying degrees of validity, depending on the specific application. Ambient density values are well-known based on atmospheric conditions; the effect of the density ratio over the given range (i.e. 250°C – 1200°C) is less than 0.5%, and the discharge coefficient is supported by literature (e.g. [8], although may vary for unusual openings). The fourth assumption becomes increasingly invalid for cases where the GER is high. Equation 9 can be reformulated to remove this assumption. This is presented in equations 10 and 11. The mass flow rate into the compartment can be shown to be a function of the opening geometry and the density variations [1]:

$$\dot{m}_a = \frac{2}{3}C_d W_v (h_0)^{\frac{3}{2}}\rho_a\sqrt{2g\frac{\rho_a-\rho_g}{\rho_a}} \tag{10}$$

$$h_0 = \frac{H_v}{1 + \sqrt[3]{\left(1 + \frac{\phi}{r}\right)^2 \frac{\rho_a}{\rho_g}}} \tag{11}$$

where W_v is the opening width, and ρ_a and ρ_g are the ambient and gas densities respectively.

Combining these equations gives:

$$\dot{m}_a = \frac{\frac{2}{3} C_d A_v \sqrt{H_v}}{\left(1 + \sqrt[3]{\left(1 + \frac{\phi}{r}\right)^2 \frac{\rho_a}{\rho_g}}\right)^{\frac{3}{2}}} \rho_0 \sqrt{2g \frac{\rho_a - \rho_g}{\rho_a}} \tag{12}$$

Applying assumptions 1-3 (taking an average over the density range) gives:

$$\dot{m}_a = \frac{2.04 A_v \sqrt{H_v}}{\left(1 + \sqrt[3]{3.4\left(1 + \frac{\phi}{r}\right)^2}\right)^{\frac{3}{2}}} \tag{13}$$

When combined iteratively with Equation 5, this allows the mass flow in and excess fuel factor to be calculated, and an updated constant can be provided for Equation 9.

Equation 13 can also be expressed as a function of pyrolysis rate, by substituting Equation 5. This gives the same result that was obtained by [9] (with temperature ratios instead of density ratios).

These formulations can be used to explore the error that results from Equation 9 as a function of GER – i.e. the error introduced by the assumption that ϕ/r is equal to zero. Figure 1 expresses the value of C as a function of GER; the relative error against the classical value of 0.5 is also plotted. For a GER of one (i.e. perfect stoichiometry) there is an error of 11% associated with Equation 1. This rises to 20% with a GER of two, and 27% with a GER of three.

Thus for application to compartment fires where significant additional pyrolysis may be expected (for example due to the presence of exposed timber surfaces), Equation 13 rather than Equation 1 must be used to obtain a more accurate estimation of mass flow rate out of the compartment (and thus GER). This requires knowledge of the pyrolysis rate.

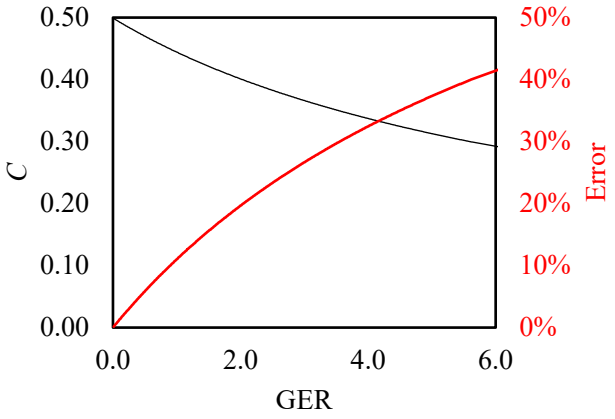

Figure 1: Error in calculation of mass flow into compartment assuming classical compartment fire theory as a function of GER.

3. Application to Compartment Fire Data

The previous sections have shown how GER can be calculated as a function of various known parameters, or measured values – i.e. compartment geometry and pyrolysis rate. In recent years, there have been several large-scale experiments and tests where the characterisation of GER is possible. In the case of large-scale fires, the direct measurement of pyrolysis rate ($\dot{m}_p$) is often not possible – instead overall heat release rate is often measured via oxygen consumption calorimetry. Consequently, to calculate GER in these experiments, a further step must be added to the calculations described in section 3. The pyrolysis rate must be estimated as a function of total heat release rate ($\dot{Q}$) and the heat of combustion of the fuel [10]:

$$\dot{m}_p = \frac{\dot{Q}}{\chi \Delta H_c} \tag{14}$$

This formulation introduces an assumption with respect to the combustion efficiency (i.e. complete combustion occurs). This assumption clearly has limitations that are worthy of further investigation. Nevertheless, it is adopted in this paper for the purposes of estimating GER in large-scale experimentation – a sensitivity study on this is presented below.

3.1. Phases of Burning

Compartment fires are typically characterised into the three phases of (1) growth (herein referred to as Phase A), (2) fully developed (Phase B), and (3) decay (Phase C) [1]. For study of compartment fires with exposed timber surfaces, it is proposed to subdivide Phase B into three further categories. Each of the phases are illustrated in Figure 2, and are described as follows and evidenced in subsequent sections.

Peak burning prior to char layer formation (Phase B1). It is known that the heat release rate of timber is highest immediately following its ignition and before the formation of a char

layer [11, 12]. For timber lined compartments (and indeed compartments with wood-based fuel loads) it follows that this will be associated to an initial peak in pyrolysis rate (and burning) which will rapidly reduce as the char layer increases in thickness.

Quasi-steady state burning of exposed timber and the compartment fuel load (Phase B2). Following the initial peak heat release rate, the pyrolysis rate of the timber becomes approximately constant [12], and the fuel is consumed as a function of the various compartment fire dynamics. This phase will therefore begin once quasi-steady state burning is achieved in the timber, and before the fuel load on the floor of the compartment has been consumed.

Quasi-steady state burning of exposed timber (Phase B3). Following the consumption of the fuel load on the compartment floor, the timber surfaces may continue to burn. In order for auto-extinction to be achieved, it is necessary for the burning rate to drop below a critical value [13]. This can only be achieved if there is a decay in the heat flux to the timber following burnout of the compartment fuel load. Hence, if continued steady-state burning of the CLT occurs after fuel burnout, auto-extinction will not be achieved. It follows from this that Phase C can exist only in the absence of Phase B3, and vice versa. It should be noted that during Phase C, continued burning of the CLT can occur; the key feature that distinguishes Phase C from Phase B3, therefore, is that Phase C may gradually decay to auto-extinction. These sequences are illustrated in Figure 2.

Once decay has begun, several paths may be followed – the fire may continue to decay, thus leading to auto-extinction [14]; or delamination may lead to an increase in HRR and possibly a secondary flashover with a potential for cyclical burning (i.e. repeated cycles of decay, delamination, and flashover) [14].

Furthermore, if some surfaces are encapsulated with gypsum plasterboard, it is possible (at any stage of the fire) that the encapsulation could fail resulting in sudden exposure of the underlying CLT, which will then ignite and contribute to the fire, characterised by a sudden increase in HRR [15, 16].

These phases allow the progression of a timber lined compartment fire to be categorised in terms of the burning behaviour. However while this approach is useful for categorising the phases of burning, it should be noted that: progression between the phases is indistinct, and therefore must be characterised by a transition period as illustrated; the exact start and end of each transition is unclear and subject to judgement; and the evolution of compartment fuel load (e.g. changes in geometry as fuel is consumed), and the possibility of delamination of CLT may lead to variation of the HRR within each phase.

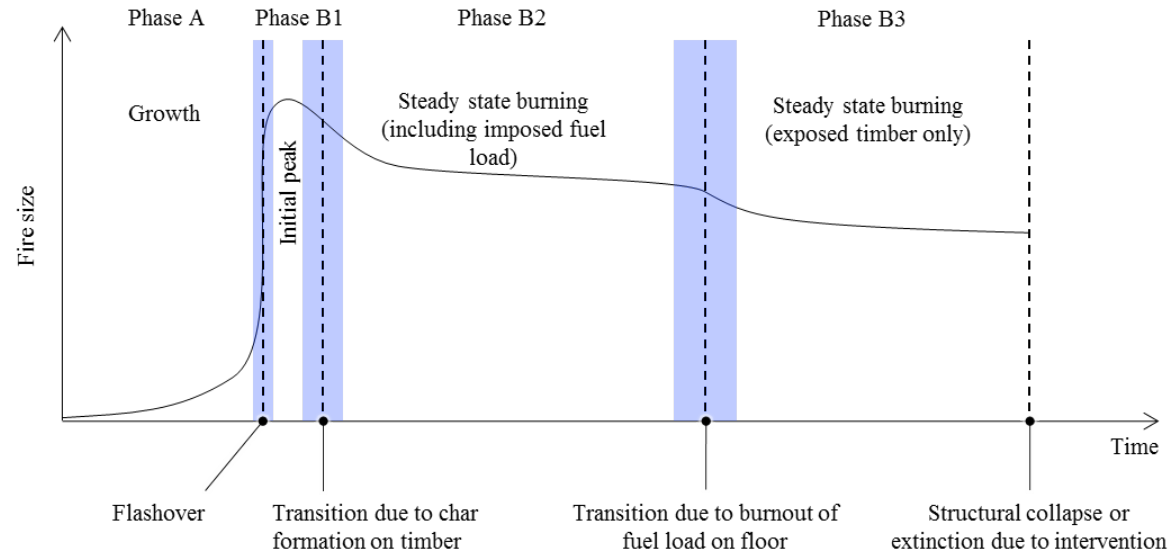

(a)

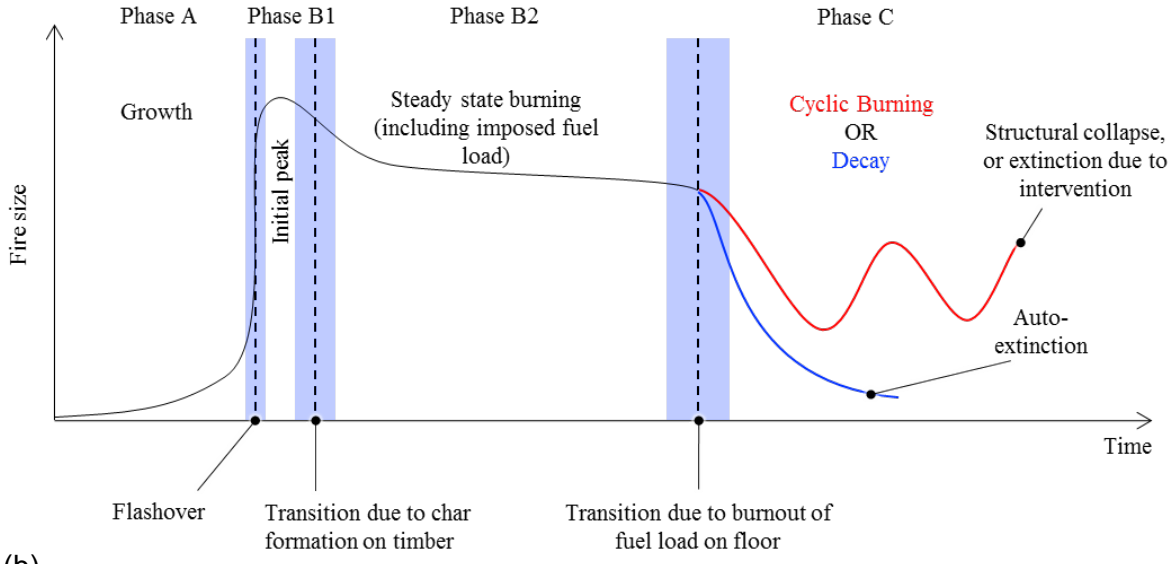

(b)

Figure 2: Illustration of different phases of burning in a compartment fire, in which (a) a steady-state burning is reached, and (b) in which decay initiates after burnout of the movable fire load.

3.1.1. Definition of Phase Transitions

In the context of reviewing the available literature [15-17], it is necessary to quantify the start and end of the various phase transitions. For the purposes of this paper, these are defined as follows.

Phase A to Phase B: This phase transition occurs at flashover, and is well-defined in literature [1], being here characterised by a sharp rise in heat release rate.

Phase B1 to Phase B2: Data from small scale experimentation by [11, 12] suggests that the burning rate changes rapidly during the first 5 minutes after ignition, and it is suggested that a quasi-steady state is achieved approximately 10 minutes after ignition for heat fluxes typical of a compartment fire. Hence 10 minutes after flashover will be used herein to define the end of this transition (if Phase B2 exists in the given case study).

Phase B2 to Phase B3: The transition from steady state burning of the imposed fuel load to burnout of the movable fuel load is not instant; hence this transition begins at the start of this decay, and ends when the mass loss of the movable fuel load is approximately zero.

Phase B to Phase C: The transition from Phase B to C is triggered by burnout of the moveable fuel load in a similar manner to above. Thus, this transition will commence at the start of the decay of the movable fuel load and end when the mass loss of the movable fuel load is approximately zero. Where burnout of the fuel load occurs less than 10 minutes after flashover, the fire will progress directly from phase B1 to C.

These phase transition definitions are not definitive, and are identified here simply to allow the existing literature [15-17] to be reviewed in a common framework.

3.2. Review of Data from Literature

In recent years, a number of studies have been made of large-scale compartment fires featuring exposed CLT within compartments:

- A series of five experiments with varying area and configurations of exposed timber were been undertaken by the University of Edinburgh [15].
- A series of large-scale compartment fire experiments, under the auspices of the Fire Protection Research Foundation, were jointly undertaken by the National Research Council (NRC), and National Institute of Standards and Technology (NIST) [16]. Computer modelling was conducted by the RISE Research Institutes of Sweden to help determine experimental parameters [17].
- Experimentation on fully and partially-exposed CLT compartment fires has also been undertaken at Carleton University [18].

It is notable that other authors have also conducted large-scale experiments on compartments with exposed timber surfaces (i.e. those without plasterboard protection) [11, 19, 20]; however, to the authors' knowledge, the experiments highlighted above are the only experiments where it is possible to make an estimation of GER using the methodology described in section 3. This is because these are the only experiments which measured and presented heat release rate data (from which mass loss rate data can be estimated).

The key geometrical data these works are summarised in Table 1. All experiments used softwood CLT with a PU adhesive. The adhesive was of brand HBE for the NRCC-NIST tests, and was not specified for the other tests.

Table 1: Summary of data from compartment fires with exposed timber surfaces.

Experiment ID	Exposed Surfaces	Width [m]	Depth [m]	Height [m]	Opening width [m]	Opening height [m]	Opening factor [$m^{1/2}$]	Fuel load [MJ/m^2]
EDI-α-1	Back wall, side wall	2.73	2.73	2.77	0.75	1.82	20.4	132 Cribs
EDI-α-2	Back wall, side wall	2.69	2.69	2.70	0.75	1.79	20.1	132 Cribs
EDI-β-1	Back wall, ceiling	2.63	2.69	2.77	0.75	1.79	20.2	132 Cribs
EDI-β-2	Back wall, ceiling	2.63	2.69	2.77	0.75	1.79	20.2	132 Cribs
EDI-γ-1	Back wall, side wall, ceiling	2.69	2.69	2.79	0.75	1.82	20.2	132 Cribs
NRCC-NIST-1-1	None	4.60	9.10	2.70	1.80	2.00	20.3	540 Furniture
NRCC-NIST-1-2	None	4.60	9.10	2.70	3.60	2.00	10.1	539 Furniture
NRCC-NIST-1-3	Side wall	4.60	9.10	2.70	3.60	2.00	10.1	549 Furniture
NRCC-NIST-1-4	Ceiling	4.60	9.10	2.70	1.80	2.00	20.3	543 Furniture
NRCC-NIST-1-5	Side wall	4.60	9.10	2.70	1.80	2.00	20.3	549 Furniture
NRCC-NIST-1-6	Side wall, ceiling	4.60	9.10	2.70	1.80	2.00	20.3	546 Furniture
Carleton	All	3.5	4.5	2.5	1.069	2	17.7	529 Furniture

The heat release data for each experiment are presented in Figure 3, broken down into the different phases identified.

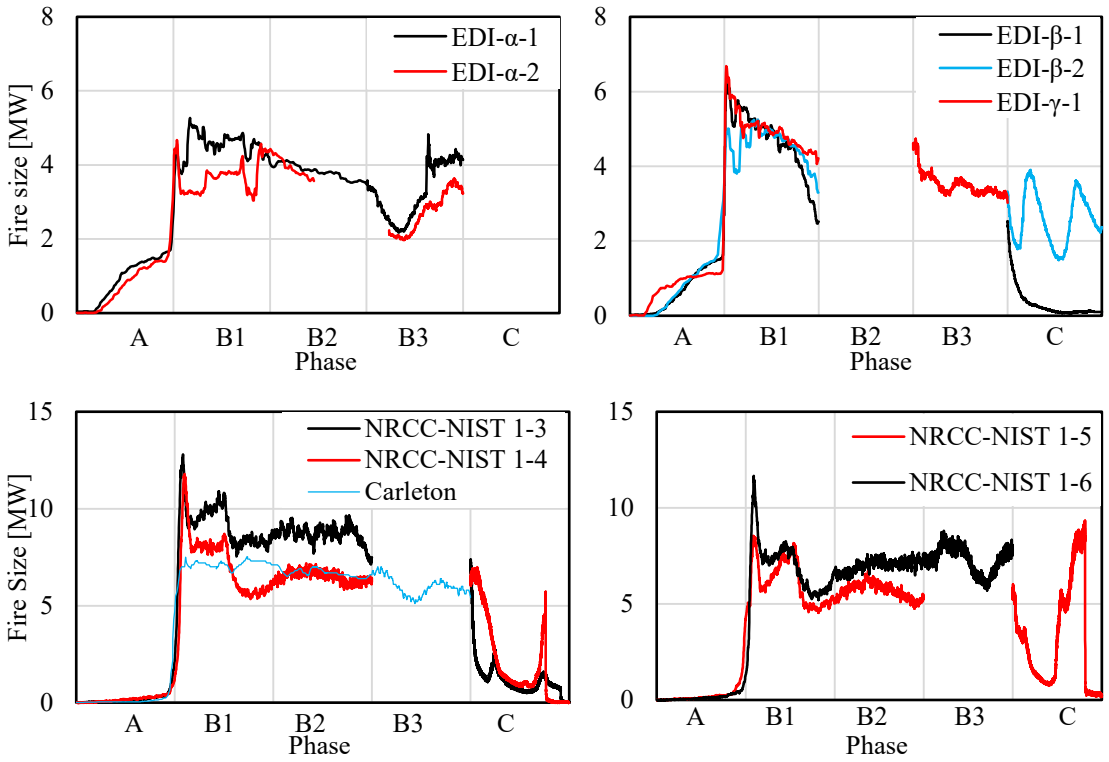

Figure 3: Heat release rate by phase of compartment fires with exposed timber surfaces in literature.

The GER for each experiment was calculated using equations 11 and 13, as shown in Figure 4. In making this calculation, it was assumed that combustion efficiency was equal to unity – these plots therefore represent a lower bound for GER (this is discussed in more detail in section 4.3.2).

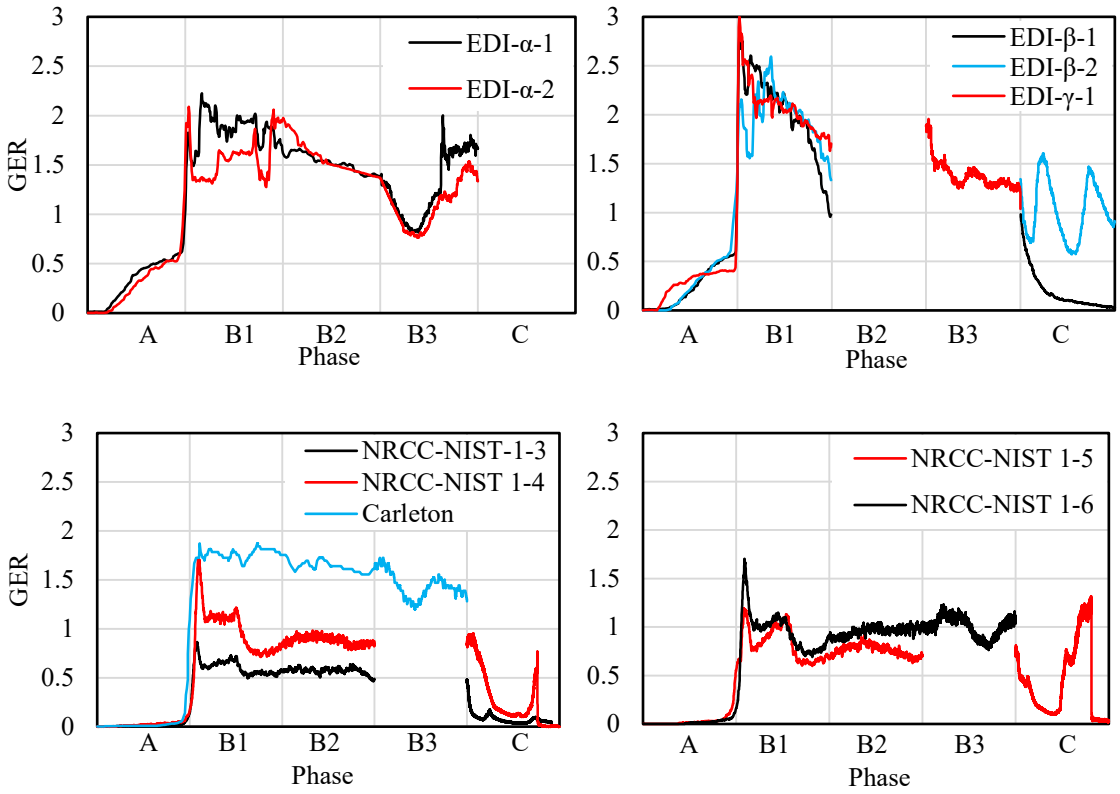

Figure 4: Global equivalence ratio by phase of compartment fires with exposed timber surfaces in literature.

Encapsulation failure was also observed in some of the experiments. For example, in experiment EDI-α-1, the encapsulation failed during phase B3, thus resulting in all CLT surfaces becoming exposed. This accounts for the high HRR and GER observed in this part of the experiment. Similarly, in NRCC-NIST tests 1-4 and 1-5 encapsulation field towards the end of the test, resulting in secondary flashover in some scenarios. This is evident from the sudden increase in HRR in Phase C of the experiments.

3.3. Analysis

3.3.1. Average GER

Three series of experiments with exposed and encapsulated (through application of gypsum plasterboard) cross-laminated timber surfaces have been analysed – from the above data, the Global Equivalence Ratios can be plotted as a function of the exposed timber. To calculate the GER for each phase (B1, B2, and B3), the phases/transitions must be defined for analysis. These are defined as follows:

Phase B1: This phase is of interest as, whilst being short in duration, will result in the highest HRR and thus GER, and therefore potentially the highest heat fluxes on the external face of the building. For this reason, the peak value was taken. This method is thus insensitive to the definition of phase transitions.

Phase B2: This phase is of interest due to the potential for long-duration, steady-state burning. The GER is thus averaged over this phase.

For the experiments undertaken by the University of Edinburgh, mass loss rate of the imposed fuel load was measured directly; the end of this phase was defined as when the mass loss rate reached zero.

For the NRCC-NIST experiments, these data were not available, and so 40 minutes was used. This was the time cited by Su *et al.* [16] for fuel burnout in an experiment with no exposed CLT. The authors have reviewed videos from the NRCC-NIST experiments, but have not been able to define more precise burnout times from these data. The value of 40 minutes was therefore adopted in the absence of other supporting data. Heat Release Rate data show that the decay in HRR starts at approximately the same time for both ventilation conditions in the unexposed scenarios, so this value has been used for both cases.

For the Carleton experiments, this transition was taken as the time described by Li *et al.* [18] as the end of the "fully-developed period".

Given the somewhat arbitrary nature of these definitions, and thus to avoid capturing too much of the transition to Phase B3 or C (and thus giving an artificially low average value for GER), the final 10% (also arbitrary) of this phase was discounted.

Phase B3: This phase is of interest due to its potential for a long-duration, steady-state burning. The first 10% of the data from the transition were again discounted, and data were used until the end of the fire (i.e. when manual suppression was applied).

The GERs for each phase are given in Table 2, alongside the Phase start/end times as defined in Section 3.1.1. It should be noted that the values provided in Table 2 provide an estimate for when the assumed global combustion efficiency is unity.

Table 2: Steady-state excess fuel factors from [15], [16], and [18].

Experiment	Peak GER	Phase B2		Phase B2 end/Phase B3 start [min]	Phase B3	
		Phase start [min]	Average GER		Average GER	Phase end [min]
EDI-α-1	2.23	14.57	1.53	17.52	1.66*	60
EDI-α-2	2.09	15.15	1.71†	20†	1.10†	60
EDI-β-1	2.82	n/a	n/a	n/a	n/a	n/a
EDI-β-2	2.60	n/a	n/a	n/a	n/a	n/a
EDI-γ-1	3.00	n/a	n/a	15.35	1.35	77.95

NRCC-NIST-1-3	0.87	22.5	0.58	37	n/a	n/a
NRCC-NIST-1-4	1.73	21.5	0.88	45	n/a	n/a
NRCC-NIST-1-5	1.19	21.5	0.77	45	n/a	n/a
NRCC-NIST-1-6	1.71	19.8	0.95	45	1.00	108.17
Carleton	1.87	20	1.65‡	25	1.41	67.2

*taken from the fall-off of plasterboard at 44 minutes, hence the moment all surfaces became exposed.

†limited data available.

‡ The GER is calculated by Li *et al.* [18] for this phase as 3.056. This is because Li makes an estimation of global combustion efficiency by dividing the total heat released by the total fuel load, resulting in a different set of assumptions to those used herein, and thus a different estimation of GER.

From the limited data available, an exposed ceiling appears to give a higher GER than an exposed wall of the same area (compare EDI-α to EDI-β). A possible source of this difference is that the pyrolysate produced from the ceiling will have a reduced mixing time with incoming oxygen compared with pyrolysate produced from the back wall. This will result in more unburned fuel exiting the compartment in the case of an exposed ceiling than for the comparable case of the back wall, thus resulting in increased burning outside the compartment. Whilst this will not change the actual value of GER (as this is related to mass loss rate), it will result in a larger external plume. Pyrolysate burned in the external plume will be subject to more efficient combustion than pyrolysate burned inside the compartment, due to greater availability of oxygen, and therefore pyrolysate burned in the external plume will result in a higher HRR than the same mass of pyrolysate burned inside the compartment. This will result in a higher HRR for an exposed ceiling than that for an exposed back wall. Therefore, the *calculated* mass loss rate (and thus the calculated GER) will be higher for the case of an exposed CLT ceiling than that of an exposed CLT back wall.

It also appears (as expected) that experiments with a lower opening factor result in a lower GER due to increased oxygen availability within the compartment, and thus reduced external flaming. As opening factor decreases further, this trend will continue, with more severe burning taking place inside the compartment, and less burning taking place in the external plume as GER decreases.

3.3.2. Sensitivity to Combustion Efficiency

The introduction of χ to calculate the pyrolysis rate introduces a significant potential error into this analysis. It is known that χ is less than 1.0 for any under-ventilated compartment fire, and that the location of the fuel within the compartment can also have an impact on combustion efficiency.

To study the sensitivity of the results to this unknown, the assumed global combustion efficiency in equation 14 was varied parametrically. This approach allowed the GER for the various scenarios described in Section 4.2 to be expressed as a function of the global combustion efficiency. Figure 5 shows the effect of assumed combustion efficiency for one experiment from each set, capturing the range of GERs across all experiments reviewed.

It is clear from this analysis that the assumed global combustion efficiency has a significant impact on the calculated values for GER, especially as the GER increases and the combustion efficiency decreases. It should be noted that for higher values of GER, more fuel will be burning outside the compartment. The external flaming will have a much greater availability of oxygen, and thus the *external plume* combustion efficiency is expected to be significantly higher than the *internal* combustion efficiency, where oxygen supply and mixing times are limited. Thus for higher values of GER, it is expected that the *global* combustion efficiency will be higher. For accurate calculation of GER in future experiments, it is thus crucial to adequately determine the combustion efficiency, or to directly measure the pyrolysis rate.

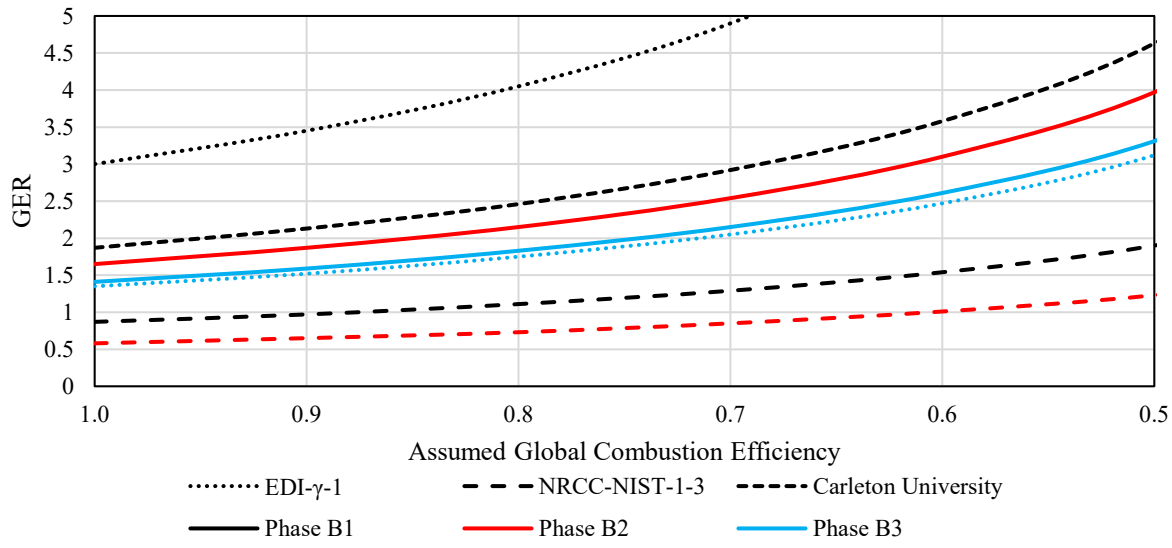

Figure 5: Global Equivalence Ratio as a function of assumed global combustion efficiency for each phase of selected experiments reviewed.

3.3.3. Development of “Burning Factor”

In classical compartment fire literature, Thomas and Heselden [21] developed the “opening factor”, $A_T/A_v\sqrt{H_v}$, which is a ratio of heat lost through the walls to heat lost through the opening. In Thomas’s opening factor uses area of the internal surfaces (A_T, excluding the floor) as a proxy for energy lost through the walls; and the parameter $A_v\sqrt{H_v}$ as a proxy for the energy lost due to convective flow through the opening. This allowed Thomas (and others) to make an energy balance to estimate temperature within the compartment.

The Global Equivalence Ratio is governed by similar parameters. The rate of pyrolysis ($\dot{m}_p$) is a function of the area of exposed fuel (A_B) (among other things), and the mass of oxygen flowing into the compartment ($\dot{m}_a m_{ox}$) has been demonstrated to be a function of the opening dimensions ($A_v\sqrt{H_v}$). It is suggested therefore, that the global equivalence ratio can correlated to a “burning factor”, and expressed as a function of A_B and $A_v\sqrt{H_v}$:

$$\phi \propto \frac{A_B}{A_v\sqrt{H_v}}$$

Where A_B represents a proxy for pyrolysis rate. Bullen and Thomas [2] made a similar observation and plotted burning rate as a function of “fuel bed area”; they indicated burning above the stoichiometric value for high fuel bed areas and/or low ventilation factors. In the case of a developing compartment fire with timber surfaces, the area of exposed fuel (and the rate at which pyrolysis occurs) varies depending on the phase of the fire. During phase B1, the burning area will include the movable fuel load and the timber surfaces (before the onset of significant charring); during phase B2 the burning area will include the movable fuel load and the compartment surfaces (after the transition to steady state); and during phase B3, the burning area will include only the timber surfaces. A_B was defined on the basis of these three phases (i.e. the floor area (to represent the imposed fuel load) and exposed walls for B1 and B2; and only exposed walls of B3). The data is plotted in Figure 6.

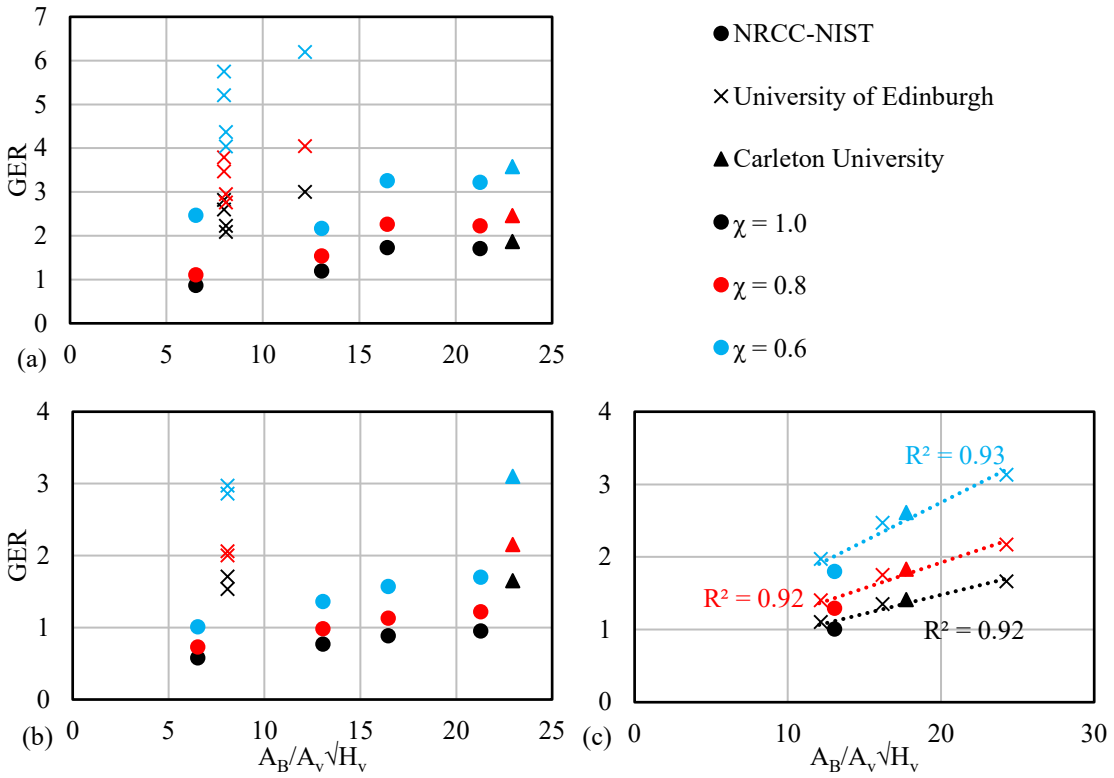

Figure 6: GER plotted for (a) Phase B1, (b) Phase B2, and (c) Phase B3 of each experiment as a function of "burning factor".

Based on this correlation for “burning factor” it is clear that there is no overall correlation for Phases B1 and B2; conversely, a very clear correlation (R^2>0.9) emerges in Phase B3. This indicates that, A_B is not a useful proxy for pyrolysis rate where there is a significant contribution of the movable fuel load. This is because the actual surface area and rate of pyrolysis of the fuel becomes more complicated when either a wood crib or real furniture is used, and is constantly changing due to parts of the fuel load being consumed. Conversely, when the when only the exposed timber surfaces are burning, the area of exposed fuel is easy to determine.

3.4. Observed bounds for GER

While the concept of a burning factor requires further investigation, particularly with regards to the definition of pyrolysis rate for complex fuel loads, the analysis presented above does allow some conclusions to be drawn about the range of possible GER for the various experimental programmes reviewed. Table 3 shows the maximum values that were obtained across all experiments reviewed as a function of combustion efficiency.

Table 3: Bounds for GER across various values of combustion efficiency.

Phase	B1	B2	B3
$\chi = 0.5$	8.40	3.97	4.01
$\chi = 0.6$	6.20	3.10	3.13

$\chi = 0.7$	4.90	2.54	2.56
$\chi = 0.8$	4.05	2.15	2.17
$\chi = 0.9$	3.45	1.87	1.88
$\chi = 1.0$	3.00	1.71	1.66

It is clear from Figure 5 and Table 3 that the assumed combustion efficiency can have a significant effect on the calculated GER. It is therefore recommended for future experiments that, where possible, the mass loss rate is measured directly to eliminate the uncertainty induced by assuming a combustion efficiency.

4. Conclusions

The additional area of fuel introduced by timber lined compartments presents a potential hazard for external fire spread. The classical simplified expression for burning rate in a compartment fire has been formulated to explicitly include Global Equivalence Ratio.

This paper has classified the phases of fully developed compartment fire with timber surfaces into three distinct phases:

- Peak burning prior to char formation (Phase B1) ;
- Quasi-steady state burning of exposed timber and the compartment fuel load (Phase B2); and
- Quasi-steady state burning of exposed timber (Phase B3).

Three sets of compartment fire experiments have been examined within this framework to estimate values of GER at different stages in the fire.

It has been found that the results are sensitive to the global combustion efficiency and this sensitivity has been quantified.

It has been found that Phase B1 is critical in terms of the maximum value of GER. No consistent difference is observed between Phase B2 and B3, although in the selected experiments the duration of Phase B2 was generally small (thereby limiting the quantitative analysis available).

For an assumed global combustion efficiency of 1.0, the maximum value of GER that was obtained was 3.00; this corresponded to a compartment with three exposed timber surfaces during phase B1. This value of GER increased to 4.05 for an assumed global combustion efficiency of 0.8.

For a compartment fire with only one exposed surface, a minimum steady-state value of 0.58 was obtained. This value of GER increased to 0.73 for a combustion efficiency of 0.8.

This represents a significant range of GER, ranging from well-ventilated conditions (NRCC-NIST-1-3), GER=0.58, to external flaming (EDI-γ-1), GER=3.00.

The concept of a “burning factor” has been developed as a possible means to correlate the results with known input parameters including explicit consideration of the ventilation conditions, as well as the area of exposed timber. It has been found that application of the burning factor, based solely on compartment geometry, provides a good correlation of GER for compartments with exposed timber surfaces after the imposed fuel load has burned out.

However, there is no apparent correlations for Phase B1 and Phase B2. This indicates that the implicit assumption that the imposed fuel load (accounted for through the proxy of floor area) and the exposed timber surfaces pyrolyse at the same rate is invalid, and thus the geometry and configuration of the imposed fuel load must be accounted for to apply the correlation in these phases.

Each of the experimental programmes analysed in this area have been primarily focussed on the internal fire dynamics and the decay (or otherwise) of the fire. In the future, to allow more detailed investigation of plume dynamics, it would be advantageous for large scale experimental programmes to gather additional data with respect to the plume. Specifically:

- To allow further investigate GER in the steady-state burning period, future large-scale experiments could use a large fuel load that prolongs the steady-state burning period; this will allow the distinction of this phase from the other phases.
- To better interpret the results from timber lined compartment experiments the combustion efficiency for timber lined compartment fires should be characterised as this has a significant impact on the resulting GER.
- Direct measurement of the global mass loss rate would allow the direct use of this parameter in calculating GER.

5. Acknowledgements

The authors gratefully acknowledge funding from EPSRC through grant EP/R012296/1. We are grateful to the authors of the pervious experimental work for publishing their data in such a manner that we were able to undertake the analyses within this paper. We are particularly grateful to Matt Hoehler and his colleagues at NIST for helpful discussions on interpretation of data from the NRCC-NIST experiments and providing us with video data of their experiments.

6. References

[1] Drysdale, D., *An introduction to fire dynamics*. 2011: John Wiley & Sons.

[2] Bullen, M.L. and P.H. Thomas, *Compartment fires with non-cellulosic fuels.* Symposium (International) on Combustion, 1979. **17**(1): p. 1139-1148.

[3] Thomas, P.H., A. Heselden, and M. Law, *Fully-developed Compartment Fires: Two Kinds of Behaviour*. 1967: HM Stationery Office.

[4] Delichatsios, M.A., et al., *Mass pyrolysis rates and excess pyrolysate in fully developed enclosure fires.* Fire Safety Journal, 2004. **39**(1): p. 1-21.

[5] Gottuk, D.T. and B.Y. Lattimer, *Effect of Combustion Conditions on Species Production*, in *SFPE Handbook of Fire Protection Engineering*, M.J. Hurley, et al., Editors. 2016, Springer New York: New York, NY. p. 486-528.

[6] Takeda, H., *Mixing effect and combustion efficiency in compartment fires.* Fire Safety Journal, 1983. **5**(3): p. 199-204.

[7] Butcher, E., G. Bedford, and P. Fardell. *Further experiments on temperatures reached by steel in building fires*. in *Proceedings of the Symposium held at the Fire Research Station, Boreham Wood*. 1967.

[8] Incropera, F. and D. DeWitt, *Fundamentals of Heat and Mass Transfer*. 5th ed. 2002, New York: John Wiley and Sons.

[9] Karlsson, B. and J. Quintiere, *Enclosure fire dynamics*. 1999: CRC press.

[10] Babrauskas, V., *Heat Release Rates*, in *SFPE Handbook of Fire Protection Engineering*, M.J. Hurley, et al., Editors. 2016, Springer New York: New York, NY. p. 799-904.

[11] Emberley, R., et al., *Description of small and large-scale cross laminated timber fire tests.* Fire Safety Journal, 2017. **91**: p. 327-335.

[12] Bartlett, A., et al., *Analysis of cross-laminated timber charring rates upon exposure to non-standard heating conditions*, in *Fire and Materials*. 2015, Interscience Communications Ltd.: San Francisco, CA. p. 667-681.

[13] Bartlett, A.I., et al., *Auto-extinction of engineered timber as a design methodology*, in *World Conference on Timber Engineering*. 2016: Vienna, Austria.

[14] Bartlett, A.I., et al., *Auto-extinction of engineered timber: Application to compartment fires with exposed timber surfaces.* Fire Safety Journal, 2017. **91**: p. 407-413.

[15] Hadden, R.M., et al., *Effects of exposed cross laminated timber on compartment fire dynamics.* Fire Safety Journal, 2017. **91**: p. 480-489.

[16] Su, J., et al., *Fire Safety Challenges of Tall Wood Buildings – Phase 2: Task 2 & 3 – Cross Laminated Timber Compartment Fire Tests*. 2018: National Research Council of Canada. p. 396.

[17] Brandon, D. and Östman, B. FPRF Project Fire Safety Challenges of Tall Wood Buildings – Phase 2, Task 2 – Test plan, modeling: The contribution of CLT to compartment fires, SP Technical Research Institute of Sweden, 2016.

[18] Li, X., et al., *Experimental Study of Combustible and Non-combustible Construction in a Natural Fire.* Fire Technology, 2014: p. 1-28.

[19] Hakkarainen, T., *Post-flashover fires in light and heavy timber construction compartments.* Journal of fire sciences, 2002. **20**(2): p. 133-175.

[20] Frangi, A. and M. Fontana. *Fire performance of timber structures under natural fire conditions*. in *Fire Safety Science Symposium*. 2005.

[21] Thomas, P.H. and A. Heselden, *Fully-developed fires in single compartments*, in *Fire Research Note*. 1972. p. 81.